Available online at www.sciencedirect.com
SCIENCE DIRECT
Journal of Molecular Catalysis A: Chemical 242 (2005) 26–31
JOURNAL OF MOLECULAR CATALYSIS A: CHEMICAL
www.elsevier.com/locate/molcata

A simple chemical synthesis of nanocrystalline AFe_2O_4 (A = Fe, Ni, Zn): An efficient catalyst for selective oxidation of styrene

Debanjan Guin, Babita Baruwati, Sunkara V. Manorama *

Materials Science Group, Indian Institute of Chemical Technology, Hyderabad 500007, India

Received 19 January 2005; received in revised form 14 July 2005; accepted 19 July 2005
Available online 24 August 2005

Abstract

Nanosized spinel ferrite (AFe_2O_4, A = Ni, Fe, Zn) catalysts are prepared by 'bottom-up' approach, i.e. first forming the nanostructured building blocks and then assembling them into the final material with average particle size of 7–12 nm and surface area of 80–100 m^2/g. The synthesized nanocrystallites were characterized by thermal analysis, powder X-ray diffraction, transmission electron microscopy and inductively coupled plasma (atomic emission spectroscopy) technique for evaluating phase, structure and morphology and stoichiometry. These materials were found to be very good catalysts for the oxidation of styrene to benzaldehyde in the presence of hydrogen peroxide. Of the several catalysts tried, magnetite (Fe_3O_4) has shown to have the best catalytic activity for the above reaction. The effects of solvent medium used, styrene:hydrogen peroxide molar ratio, reaction temperature, time and reaction atmosphere required for the complete conversion of styrene to benzaldehyde were also studied. Based on our findings, a plausible mechanism involved in the catalytic reaction is proposed.

Keywords: Nanoparticles; Spinel ferrites; Catalyst; Styrene; Oxidation

1. Introduction

Nanospinel ferrites with the general formula AB_2O_4 are a class of chemically and thermally stable materials suitable for a wide variety of applications including catalysis [1], magnetic recording media and magnetic fluids for the storage and/or retrieval of information [2], magnetic resonance imaging (MRI) enhancement [3], magnetically guided drug delivery [4], sensors [5], pigments [6], etc. It is established that various binary and ternary spinel ferrites are effective catalysts for a number of industrial processes such as oxidative dehydrogenation of hydrocarbons [7], decomposition of alcohols and hydrogen peroxide [8], treatment of automobile-exhaust gases [9], oxidation of various compounds such as CO [10], H_2, CH_4 and chlorobenzene [11], phenol hydroxylation [12], alkylation reaction [13], hydrodesulphurization of crude petroleum [14], catalytic combustion of methane [15], etc.

Synthesis procedures of these spinel ferrite nanoparticles have also been intensively studied in recent years. Large-scale application of ferrites with small particles and tailoring of specific properties have prompted the development of several widely used chemical methods [16] like sol–gel [17], radio frequency plasma treatment [18], reverse micelles [19], host template [20], co-precipitation [21], hydrothermal treatment [22], etc. Among these techniques, hydrothermal synthesis is a method with an advantage that it can be easily operated and produces large quantities of nanostructured material in a comparatively less time. The main thrust of research in this area is exploring synthesis routes involving minimum temperature, to minimize the grain growth associated with high temperature treatment. The physicochemical properties and catalytic performance of these materials in the selective oxidation of styrene with H_2O_2 as oxidant to form benzaldehyde, targeting the fine chemical industry, has been addressed.

2. Experimental

2.1. Synthesis of the catalysts

Among the catalysts used for the reaction, $NiFe_2O_4$, $ZnFe_2O_4$ and $Ni_{0.5}Zn_{0.5}Fe_2O_4$ are synthesized by the hydrothermal route whereas Fe_3O_4 was synthesized at room temperature.

* Corresponding author. Tel.: +91 40 27160123x2386; fax: +91 40 27160921.
E-mail address: manorama@iict.res.in (S.V. Manorama).

1381-1169/$ – see front matter © 2005 Elsevier B.V. All rights reserved.
doi:10.1016/j.molcata.2005.07.021

The synthesis procedures can be described briefly as follows.

2.1.1. Synthesis of $NiFe_2O_4$, $ZnFe_2O_4$ and $Ni_{0.5}Zn_{0.5}Fe_2O_4$

Stoichiometric amounts of $Ni(NO_3)_2{\cdot}6H_2O$, $Zn(NO_3)_2$ and $Fe(NO_3)_3{\cdot}9H_2O$ are dissolved in doubly distilled water. The pH of the solution was adjusted to 8 by slow addition of ammonia solution. The reaction mixture was stirred for 1 h before transferring the contents to a 1000 ml stainless steel autoclave. The temperature of the autoclave was maintained at 230 °C for half an hour and then the reaction mixture was allowed to cool to room temperature. The product formed was washed with distilled water several times, filtered and dried at 100 °C for 8 h. Similarly, $NiFe_2O_4$ was also synthesized while maintaining pH of the starting composition at 10.

2.1.2. Synthesis of Fe_3O_4

Fe_3O_4 is synthesized at room temperature using hydrazine monohydrate. In a typical synthesis process, $FeCl_2$ (Aldrich) was dissolved in doubly distilled water, acidified with HCl during continuous stirring at ambient temperature and pressure to obtain a clear solution. Hydrazine monohydrate ($N_2H_4{\cdot}H_2O$) was used to adjust the pH of the solution to almost 7. During this process of addition, it was observed that the solution that was originally dark green in color (phase identified as green rust) changed to black indicative of the formation of Fe_3O_4 and completion of the reaction. The reaction mixture was stirred for a further period of 1 h and the black precipitate was collected, filtered and repeatedly washed with distilled water. The product was subsequently dried in vacuum for 2 h at room temperature.

2.2. Characterization

Powder X-ray diffraction (XRD) was recorded on a Siemens/D5000 X-ray diffractometer over a 2θ range from 2° to 65° using Cu Kα ($\lambda = 1.5406$ Å). The thermal transformations associated with the heat treatment were studied by a thermogravimetric-differential thermal analysis (TG-DTA) system (Model: Mettler Toledo Star^e) in air, at a heating rate of 10 °C/min. A JEOL JEM–200 CX transmission electron microscope operating at 200 kV was used to record the selected area electron diffraction (SAED) and the transmission electron microscopy (TEM) patterns. An IRIS Intrepid II XDL inductively coupled plasma, atomic emission spectroscopy (ICP-AES) instrument was used to measure the stoichiometry of the samples.

2.3. Reaction procedure for the oxidation of styrene

Styrene oxidation was carried out in a 50 ml two-necked round bottom flask provided with a magnetic bead for stirring and a flask condenser; 10 mmol styrene, 10 ml acetone, 0.1 g catalyst and 1 ml of 30 wt% H_2O_2 (styrene:H_2O_2 = 1) were added successively into the flask. The reaction was carried out with varying solvents, temperature, time, styrene:H_2O_2 molar ratio and reaction atmosphere. The reaction products were analyzed by gas chromatographic mass spectroscopy (GCMS) at regular intervals. At temperatures above 60 °C and reaction time greater than 12 h, the formation of styrene polymers was observed. The optimum condition for the reaction was obtained using acetone as solvent at 60 °C for a 12 h reaction period.

3. Results and discussions

At the outset all the catalyst materials were characterized for evaluating their morphology and structure. The synthesized samples were first subjected to thermal analysis to find out the possible temperatures at which any possible phase change could occur.

3.1. Thermal analysis

Thermal analysis of the as-prepared samples was done to know the possible changes occurring when they are subjected to heat treatment. From TG-DTA studies it is seen that the data for the hydrothermally synthesized ferrites is featureless in the temperature range from 30 to 350 °C, except for the water loss peak near 100 °C. Near 350 °C, there is an endothermic peak indicating total crystallization for the samples synthesized at pH 8. For the $NiFe_2O_4$ sample synthesized at pH 10, the whole data is featureless indicating that no phase change occurs up to the temperature of interest. However for Fe_3O_4 synthesized at room temperature, as expected, there are two peaks at 240 and 450 °C showing the phase transformations which can be assigned to the phase change of magnetite to maghemite and then to hematite, respectively [23]. The maximum gravimetric loss accompanying this thermal treatment was found to be around 8%, which is mainly due to loss of water. The TG-DTA plots for Fe_3O_4 and the other complex ferrites are given in Figs. 1 and 2.

3.2. Powder X-ray diffraction

X-ray diffraction studies indicate that the materials synthesized are spinels with the cubic phase and all the crystal structures agree with the corresponding reported JCPDS data (Card Nos. $NiFe_2O_4$: 10-325; $ZnFe_2O_4$: 22-1012; Fe_3O_4: 19-629). Fig. 3 shows the powder XRD patterns of all the materials. A definite line broadening of the diffraction peaks is an indication that the synthesized materials are in the nanometer range. The crystallite sizes are calculated from Debye Scherrer formula applied to the major intense peaks and are found to be in the range of 10–15 nm. The lattice parameters calculated are also in accordance with the reported value. All the crystal parameters are given in Table 1.

3.3. Transmission electron microscopy

Figs. 4 and 5 give the TEM micrographs of the complex ferrites and Fe_3O_4 nanoparticles, respectively. The corresponding SAED pattern for the Fe_3O_4 particles are also given in Fig. 5. The average particle size calculated from the TEM micrographs is consistent with the crystallite size obtained from XRD measurement and is included in Table 1. This also indicates that the

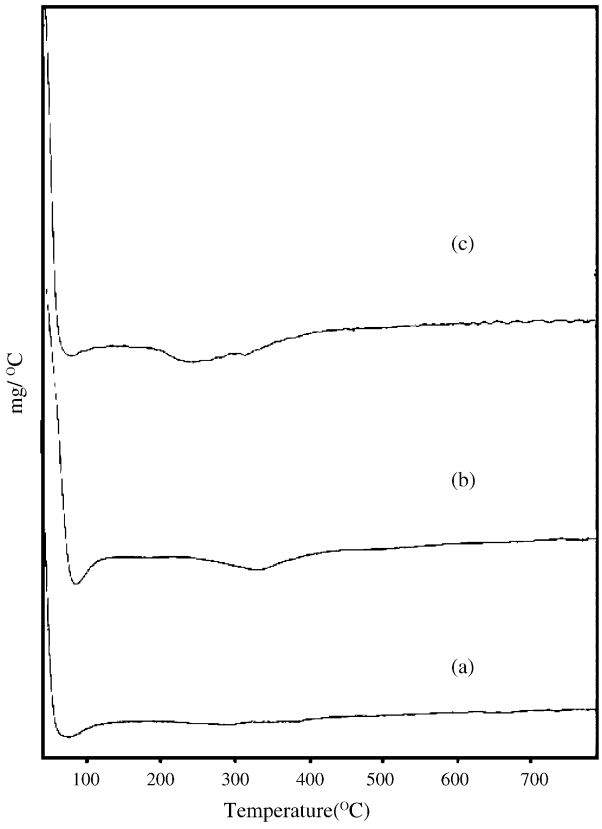

Fig. 1. Differential thermal analysis plot of (a) $NiFe_2O_4$, (b) $ZnFe_2O_4$, (c) $Ni_{0.5}Zn_{0.5}Fe_2O_4$ synthesized by hydrothermal treatment at 230 °C for half an hour.

synthesis procedure adopted results in particles that mostly very small and nearly single crystals.

From ICP studies it is found that all the samples have an (A = Fe, Ni and Zn): Fe^{3+} ratio equal to 1:2 with an error less than 3%.

3.4. Optimization of reaction conditions

The materials thus characterized for the structure, morphology and confirmed to be nanomaterials with the spinel structure were then used as catalysts to evaluate their catalytic efficiency. The oxidation reaction of styrene to benzaldehyde was used as the model reaction. The effect of different solvents, temperature

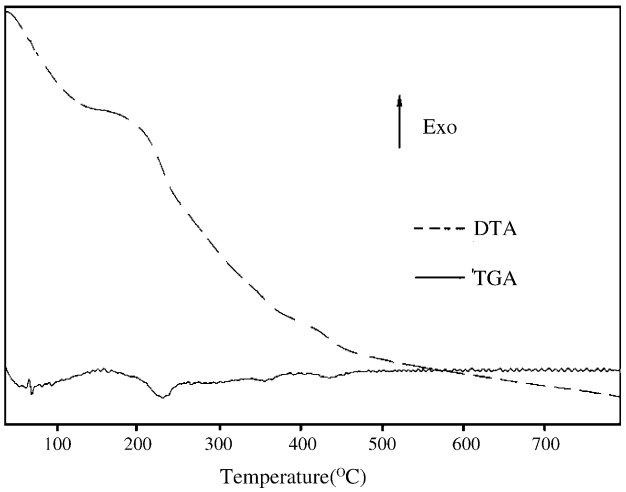

Fig. 2. DTA-TGA plot of room temperature synthesized Fe_3O_4.

variation, styrene:H_2O_2 molar ratio, reaction atmosphere, etc. on the styrene conversion and product selectivity over AFe_2O_4 (A = Fe, Ni and Zn) and $A_{0.5}B_{0.5}Fe_2O_4$ (A = Ni, B = Zn) type catalysts have been successively carried out. $NiFe_2O_4$ prepared at pH 8 shows 31.4 mol% conversion and 55.6 mol% benzaldehyde selectivity where as $NiFe_2O_4$ synthesized at pH 10 shows only 24.0 mol% conversion and 36.5 mol% selectivity. Preparing the same material at different pHs is justified, based on our early work where it is shown that the procedure adopted confirms different electrical conductivity behavior [24]. In $NiFe_2O_4$ this effect primarily arises from the presence of different Ni species (Ni^{2+} and Ni^{3+}). We can therefore ascribe the lower value of conversion and selectivity in the case of $NiFe_2O_4$, prepared at pH 10 to less oxygen vacancies in the active sites of the catalyst. $ZnFe_2O_4$ and $Ni_{0.5}Zn_{0.5}Fe_2O_4$ have shown 26.1 and 30.7 mol% conversion and with a benzaldehyde selectivity of 50.4 and 52.1 mol%, respectively. The styrene conversion with these catalysts has shown no significant change. Using all these catalysts and also Fe_3O_4, styrene oxidation reactions are carried out at 60 °C with acetone as the solvent for 12 h reaction in nitrogen atmosphere and the results are tabulated in Table 2. The best result in terms of conversion of styrene is 36.5 mol% and benzaldehyde selectivity of 68.4 mol% is obtained using Fe_3O_4 catalysts. The primary reason for the improved catalytic efficiency of Fe_3O_4 can be attributed to the pH that is adjusted

Table 1
Synthesis conditions; results from XRD, crystallite size and diffused reflectance spectroscopy of the nanoparticles of AFe_2O_4 (A = Fe, Ni, Zn and $Ni_{0.5}Zn_{0.5}$) complex oxides

Code	T (°C)	Time (h)	Crystallite size[a] (nm)	Average surface area[b] (m^2/g)	Lattice parameter[c] (Å)	Particle size[d] (nm)
$NiFe_2O_4$ (pH 8)	230	0.5	9.3	100.9	8.37	10–12
$NiFe_2O_4$ (pH 10)	230	0.5	9.2	85.4	8.40	12–15
$ZnFe_2O_4$	230	0.5	8.2	111.0	8.40	8–13
$Ni_{0.5}Zn_{0.5}Fe_2O_4$	230	0.5	7.9	100.9	8.45	9–11
Fe_3O_4 (pH 7)	26	1	15	55.51	8.30	18–22

[a] From XRD.
[b] Calculated from TEM.
[c] Calculated from Scherrer formula.
[d] Calculated from TEM micrograph.

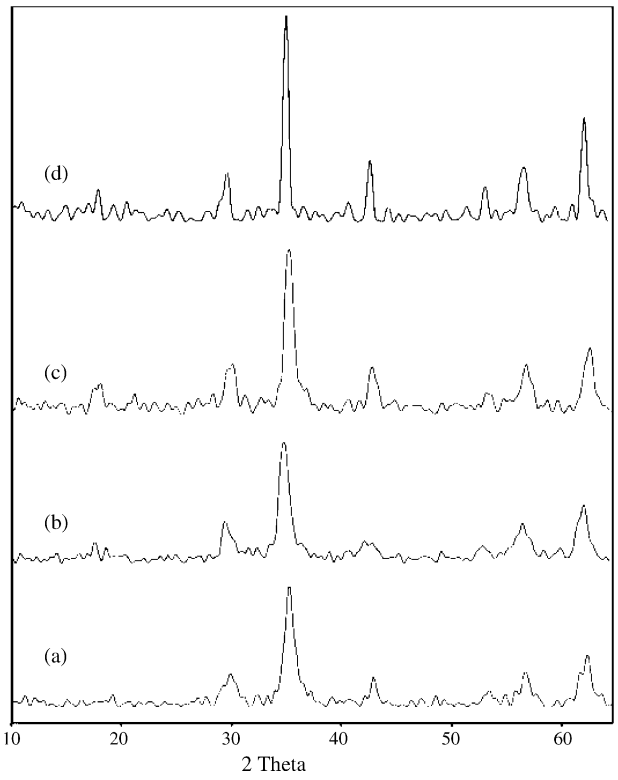

Fig. 3. Powder X-ray diffraction patterns of (a) $ZnFe_2O_4$, (b) $NiFe_2O_4$ (pH 8), (c) $Ni_{0.5}Zn_{0.5}Fe_2O_4$ and (d) Fe_3O_4.

at 7 during the synthesis procedure. For others, the pH value during synthesis was maintained at 8 and above to obtain single phase compound. The lower pH value (pH 7) maintained during the synthesis of Fe_3O_4 leads to more oxygen vacancies on the surface. More oxygen vacancies facilitate the adsorption of H_2O_2 to form molecular oxygen for the oxidation reaction compared to the other catalysts studied and hence we observe a better promotion of the oxidation procedure. Further, this preferential enhancement may be due to the variable valencies of iron, existing in the Fe_3O_4. In an equilibrium situation, this favors the simultaneous oxidation of Fe^{2+} to Fe^{3+} along with the cleavage of the double bond in styrene on the Fe^{3+} surface. Thus, the presence of both Fe^{2+} and Fe^{3+} ions in Fe_3O_4 favors the adsorption of both reactants, i.e. H_2O_2 and styrene together thereby contributing to the enhanced catalytic activity in this material. In the case of the other catalysts, $NiFe_2O_4$ and $ZnFe_2O_4$, also with the spinel structure, the adsorption processes are less advantageous as Ni and Zn ions prefer the divalent oxidation state and it is Fe^{2+} ions that are replaced by Ni^{2+} and Zn^{2+} ions, respectively. These reasons support the experimental result which show that using Fe_3O_4 catalyst one would expect better styrene conversion (36.5%) and higher benzaldehyde selectivity (68.4%) under optimum conditions.

Table 2
Oxidation of styrene with H_2O_2 with all the synthesized complex ferrite catalysts

Catalyst	Styrene conversion (mol%)	Selectivity (mol%)	
		Benzaldehyde	Others
$NiFe_2O_4$ (pH 8)	31.4	55.6	33.4
$NiFe_2O_4$ (pH 10)	24.0	36.5	40.8
$ZnFe_2O_4$	26.1	50.4	36.5
Fe_3O_4 (pH 7)	36.5	68.4	32.1
$Ni_{0.5}Zn_{0.5}Fe_2O_4$	30.7	52.1	42.0

Reaction conditions: catalyst 0.1 g; solvent acetone; styrene:H_2O_2 molar ratio 1; reaction temperature 60 °C; 12 h reaction N_2 atmosphere.

The influence of reaction temperature, time and styrene:hydrogen peroxide molar ratio on the styrene oxidation reaction is given in Table 3. With the increase in reaction temperature, styrene conversion as well as the selectivity for benzaldehyde increases. This confirms that at higher temperatures C=C bond cleavage is more favorable. It is seen that the styrene conversion increases with the increase in reaction time but selectivity for benzaldehyde decreases, and the formation of other products like polystyrene, etc. increases. The conversion as well as the selectivity is found to be best when the styrene:hydrogen peroxide molar ratio is 1:1 and the reaction time is 12 h. When styrene:hydrogen peroxide molar ratio is 1:2, it is seen that the styrene conversion increases but the product selectivity decreases. When this ratio is maintained at 2:1, the styrene conversion decreases but the selectivity for benzaldehyde increases. So we can conclude that the optimum

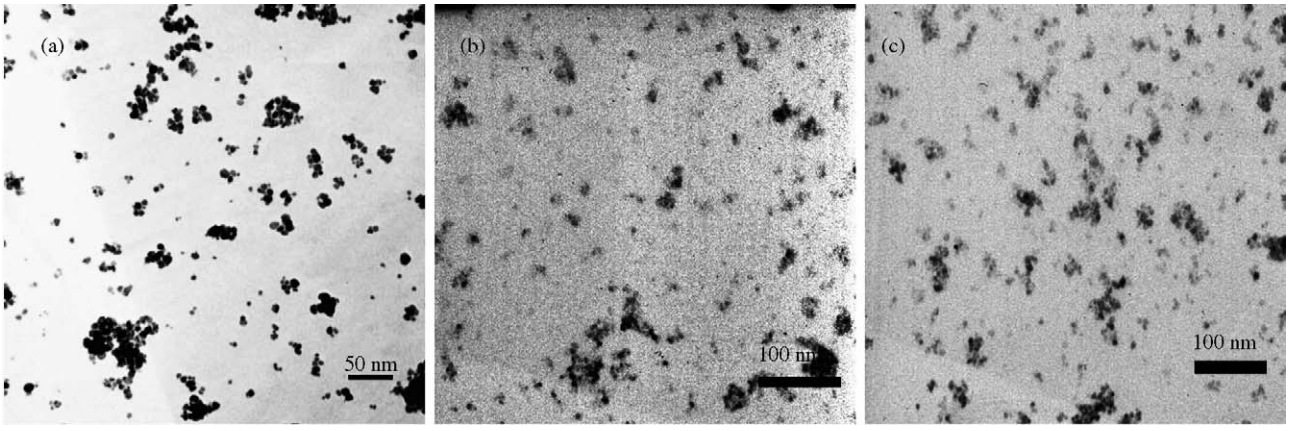

Fig. 4. Typical transmission electron micrographs of all the samples showing the particle size distribution (a) $ZnFe_2O_4$, (b) $NiFe_2O_4$ and (c) $Ni_{0.5}Zn_{0.5}Fe_2O_4$.

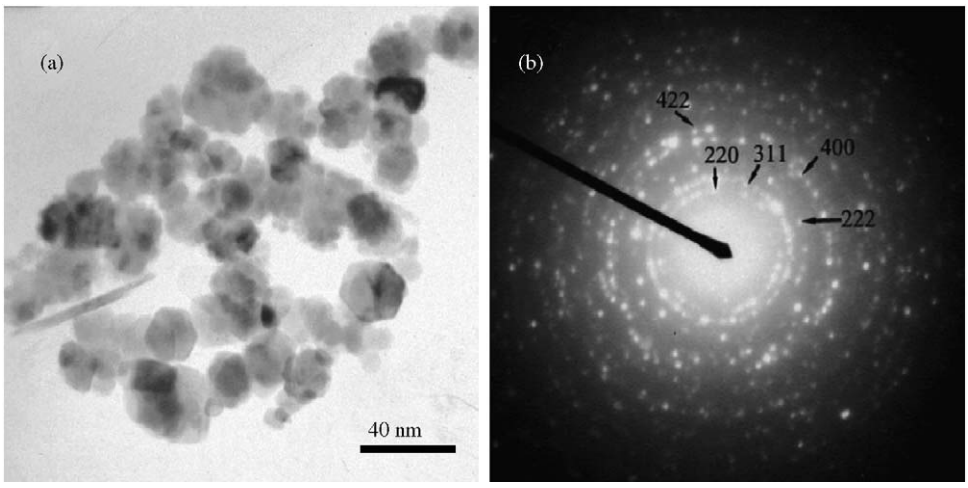

Fig. 5. Typical transmission micrographs and selected area electron diffraction pattern of Fe_3O_4 showing the particle size.

Table 3
Effect of reaction temperature, reaction time and styrene:H_2O_2 molar ratio on styrene oxidation on Fe_3O_4 catalyst

Temperature (°C)	Time (h)	Styrene:H_2O_2 molar ratio	Styrene conversion (mol%)	Selectivity (mol%)	
				Benzaldehyde	Others
30	12	1:1	2.1	70.6	25.1
40	12	1:1	10.1	66.6	29.3
50	12	1:1	19.0	63.2	30.2
60	12	1:1	36.5	68.4	32.1
60	6	1:1	1.3	72.3	19.5
60	18	1:1	52.0	51.0	36.2
60	24	1:1	55.2	24.8	64.8
60	12	1:2	36.5	44.6	30.2
60	12	2:1	5.8	72.1	25.8

Reaction conditions: catalyst 0.1 g; N_2 atmosphere; acetone solvent.

conversion is obtained when this molar ratio is 1:1. Further, the influence of different solvent and reaction atmospheres has also been studied on this reaction.

The results obtained with different solvents and atmospheres on styrene oxidation over 0.1 g Fe_3O_4 catalyst at 60 °C keeping styrene:hydrogen peroxide molar ratio as 1:1 and 12 h reaction time is given in Table 4. From the table it is clear that aprotic solvents like acetone, acetonitrile, etc. are more favorable than protic solvents for the formation of benzaldehyde. Though no significant change in conversion and selectivity of the reaction is observed, N_2 atmosphere seems to be more favorable than air or O_2 atmosphere for performing the reaction. This could probably be because in air or oxygen atmosphere there is a possibility for styrene to be polymerized hindering the reaction pathway.

Table 4
Effect of solvent and reaction atmosphere on styrene oxidation over Fe_3O_4 catalyst

Solvent	Reaction atmosphere	Styrene Conversion (mol%)	Selectivity (mol%)	
			Benzaldehyde	Others
Acetone	N_2	31.22	71.0	26.4
Acetone	O_2	24.0	52.8	31.2
Acetone	Air	25.1	55.3	32.5
Ethanol	N_2	26.6	48.9	38.9
Acetonitrile	N_2	25.4	52.3	38.5

Reaction conditions: catalyst 0.1 g; temperature 60 °C; styrene:H_2O_2 molar ratio 1; time 12 h.

4. Conclusions

The following are the inferences that can be drawn from the above studies:

1. Nanosized spinel-type AFe_2O_4 (A = Ni, Zn and $Ni_{0.5}Zn_{0.5}$) complex oxide catalysts are prepared by the hydrothermal method. These complex type ferrite catalysts are found to be highly active for the oxidation of styrene with H_2O_2 oxidant due to their high dispersity, and large surface area, i.e. providing more active sites for the catalytic reaction.
2. Styrene undergo a C=C bond cleavage preferentially over the spinel-type catalysts to give benzaldehyde. By-products such as phenylacetaldehyde and styrene oxide formation are negligibly low (<1%).
3. Among all complex ferrites, Fe_3O_4, synthesized at around pH 7, is found to be most effective for styrene oxidation to benzaldehyde. This may be due to large number of oxygen vacancies on the surface among the ferrites studied.

4. With acetone as the reaction medium, reaction temperature around 60 °C, reaction time 12 h and styrene:hydrogen peroxide molar ratio 1:1 under nitrogen atmosphere is found to be favorable for increasing the selectivity for benzaldehyde.

Thus, we can conclude that most favorable conditions for the oxidation of styrene to benzaldehyde is obtained with Fe_3O_4 as a catalyst, acetone as the reaction medium and reaction temperature maintained at 60 °C for 12 h.

Acknowledgements

Authors are thankful to DST, New Delhi, for the financial support, B.B. acknowledges CSIR and D.G. acknowledges DST, New Delhi, for the Research Fellowship.

References

[1] N. Ma, Y. Yue, W. Hua, Z. Gao, Appl. Catal. A: Gen. 251 (2003) 39.
[2] M.H. Kryder, Mater Res. Soc. Bull. 21 (1996) 9.
[3] D.G.H. Mitchell, J. Magn. Reson. Imaging 7 (1997) 1.
[4] S.P. Bhatnagar, R.E. Rosensweig, J. Magn. Magn. Mater. 149 (1995) 198.
[5] L. Satyanarayana, K.M. Reddy, S.V. Manorama, Sens. Actuators B 89 (2003) 62.
[6] R.A. Canderia, M.I.B. Bernardi, E. Longo, I.M.G. Santosh, A.G. Souza, Mater. Lett. 58 (2004) 569.
[7] M.A. Gibson, J.W. Hightower, J. Catal. 41 (1976) 420.
[8] E. Manova, T. Tsoncheva, D. Paneva, I. Mitov, K. Tenchev, L. Petrov, Appl. Catal. A: Gen. 277 (2004) 119.
[9] L.C.A. Oliveira, J.D. Fabris, R.R.V.A. Rios, W.N. Mussel, R.M. Lago, Appl. Catal. A: Gen. 259 (2004) 253.
[10] S. PalDey, S. Gedevanishvii, W. Zhang, F. Rasouli, Appl. Catal. B: Environ. 56 (2004) 227.
[11] J.B. Silva, C.F. Diniz, R.M. Lago, N.D.S. Mohallem, J. Non-Cryst. Solids 348 (2004) 201.
[12] C.R. Xiong, Q.L. Chen, W.R. Lu, H.X. Gao, W.K. Lu, Z. Gao, Catal. Lett. 69 (2000) 231.
[13] K. Sreekumar, S. Sugunan, J. Mol. Catal. A: Chem. 185 (2002) 259.
[14] F. Tihay, A.C. Roger, G. Pourroy, A. Kiennemann, Energy Fuels 16 (2002) 1271.
[15] R. Spretz, S.G. Marchetti, M.A. Ulla, E.A. Lombardo, J. Catal. 194 (2000) 167.
[16] T. Hyeon, Chem. Commun. 8 (2003) 927.
[17] W. Stober, A. Fink, E.J. Bohn, Colloid Interface Sci. 26 (1968) 62.
[18] S. Son, M. Taheri, E. Carpenter, V.G. Harris, M.E. McHenry, J. Appl. Phys. 91 (2003) 10.
[19] N. Mounien, M.P. Pileni, Langmuir 13 (1997) 3927.
[20] N.S. Kommareddi, M. Tata, V.T. Jhon, G.L. McPherson, M.F. Herman, Chem. Mater. 8 (1996) 801.
[21] M.F.F. Lelis, A.O. Porto, C.M. Goncalves, J.D. Fabris, J. Magn. Magn. Mater. 278 (2003) 263.
[22] S. Komarneni, M.C. D'Arrigo, C. Leonelli, G.C. Pellacani, H. Katsuki, J. Am. Ceram. Soc. 81 (1998) 11.
[23] J. Tang, M. Myers, K.A. Bosnick, L.E. Brus, J. Phys. Chem. B 107 (2003) 7501.
[24] B. Baruwati, K.M. Reddy, S.V. Manorama, R.K. Singh, Om Parkash, Appl. Phys. Lett. 85 (2004) 2833.